Toxicology Letters 205 (2011) 302–309

Contents lists available at ScienceDirect

Toxicology Letters

journal homepage: www.elsevier.com/locate/toxlet

Photoirradiation of dehydropyrrolizidine alkaloids—Formation of reactive oxygen species and induction of lipid peroxidation☆

Yuewei Zhao[a], Qingsu Xia[a], Jun Jie Yin[b], Ge Lin[c], Peter P. Fu[a,*]

[a] National Center for Toxicological Research, U.S. Food and Drug Administration, Jefferson, AR 72079, USA
[b] Center for Food Safety and Applied Nutrition, U.S. Food and Drug Administration, College Park, MD 20740, USA
[c] School of Biomedical Sciences, The Chinese University of Hong Kong, Hong Kong, China

ARTICLE INFO

Article history:
Received 2 March 2011
Received in revised form 14 June 2011
Accepted 15 June 2011
Available online 22 June 2011

Keywords:
Dehydropyrrolizidine alkaloids
Photoirradiation
UVA light
Reactive oxygen species
Lipid peroxidation

ABSTRACT

Pyrrolizidine alkaloid (PA)-containing plants are widespread in the world and are probably the most common poisonous plants affecting livestock, wildlife, and human. PAs require metabolic activation to generate pyrrolic metabolites (dehydro-PAs) that bind cellular protein and DNA, leading to hepatotoxicity and genotoxicity, including tumorigenicity. In this study we report that UVA photoirradiation of a series of dehydro-PAs, e.g., dehydromonocrotaline, dehydroriddelliine, dehydroretrorsine, dehydrosenecionine, dehydroseneciphylline, dehydrolasiocarpine, dehydroheliotrine, and dehydroretronecine (DHR) at 0–70 J/cm^2 in the presence of a lipid, methyl linoleate, resulted in lipid peroxidation in a light dose–responsive manner. When irradiated in the presence of sodium azide, the level of lipid peroxidation decreased; lipid peroxidation was enhanced when methanol was replaced by deuterated methanol. These results suggest that singlet oxygen is a photo-induced product. When irradiated in the presence of superoxide dismutase, the level of lipid peroxidation decreased, indicating that lipid peroxidation is also mediated by superoxide. Electron spin resonance (ESR) spin trapping studies confirmed that both singlet oxygen and superoxide anion radical were formed during photoirradiation. These results indicate that UVA photoirradiation of dehydro-PAs generates reactive oxygen species (ROS) that mediated the initiation of lipid peroxidation. UVA irradiation of the parent PAs and other PA metabolites, including PA *N*-oxides, under similar experimental conditions did not produce lipid peroxidation. It is known that PAs induce skin cancer and are secondary (hepatogenous) photosensitization agents. Our results suggest that dehydro-PAs are the active metabolites responsible for skin cancer formation and PA-induced secondary photosensitization.

Published by Elsevier Ireland Ltd.

1. Introduction

Pyrrolizidine alkaloids (PAs) are hepatotoxic and tumorigenic phytochemicals present in twelve higher plant families of the Angiosperms (Fu et al., 2002, 2004, 2010; IPCS, 1989; Mattocks, 1986). It has been reported that about 3% of the world's flowering plants contain toxic PAs (Smith and Culvenor, 1981). To date, more than 660 PAs and PA *N*-oxides have been identified in over 6000 plants grown worldwide, and about half of them are hepatotoxic. Toxic PA-containing plants grow in South Africa, Central Africa, the West Indies, China, Jamaica, Canada, Europe, New Zealand, Australia, and the United States. It is highly possible that PA-containing plants are the most common poisonous plants affecting livestock, wildlife, and humans (Fu et al., 2002, 2004; IARC, 1976; Li et al., 2008; Mattocks, 1986; Roeder, 1995, 2000; WHO, 1988). There are a number of PAs that have been found to induce tumors in experimental animals (Fig. 1) (Fu et al., 2002, 2004; Mattocks, 1986). In 1989, the International Programme on Chemical Safety (IPCS) determined that PAs are a threat to human health and safety (IPCS, 1989).

PAs require metabolic activation to exert toxicities. The metabolic activation pathways leading to hepatotoxicity and genotoxicity have been extensively studied (Fu et al., 2002, 2004, 2007, 2010; Li et al., 2008; Zhou et al., 2010). Using riddelliine as an example, there are three principal metabolic pathways (Fig. 2). The first pathway is hydrolysis of the ester group to form retronecine. The second pathway is *N*-oxidation of the necine base to form riddelliine *N*-oxide, which may undergo reduction and be converted back to riddelliine. The third metabolic pathway is oxidation to form dehydroriddelliine, a pyrrolic ester. Pyrrolic metabolites

Abbreviations: PA, pyrrolizidine alkaloid; DHP, (±)6,7-dihydro-7-hydroxy-1-hydroxymethyl-5*H*-pyrrolizine; DHR, dehydroretronecine or (−)*R*-6,7-dihydro-7-hydroxy-1-hydroxymethyl-5*H*-pyrrolizine; NCTR, National Center for Toxicological Research.

☆ This article is not an official US Food and Drug Administration (FDA) guidance or policy statement. No official support or endorsement by the US FDA is intended or should be inferred.

* Corresponding author. Tel.: +1 870 543 7207; fax: +1 870 543 7136.
E-mail address: peter.fu@fda.hhs.gov (P.P. Fu).

0378-4274/$ – see front matter Published by Elsevier Ireland Ltd.
doi:10.1016/j.toxlet.2011.06.020

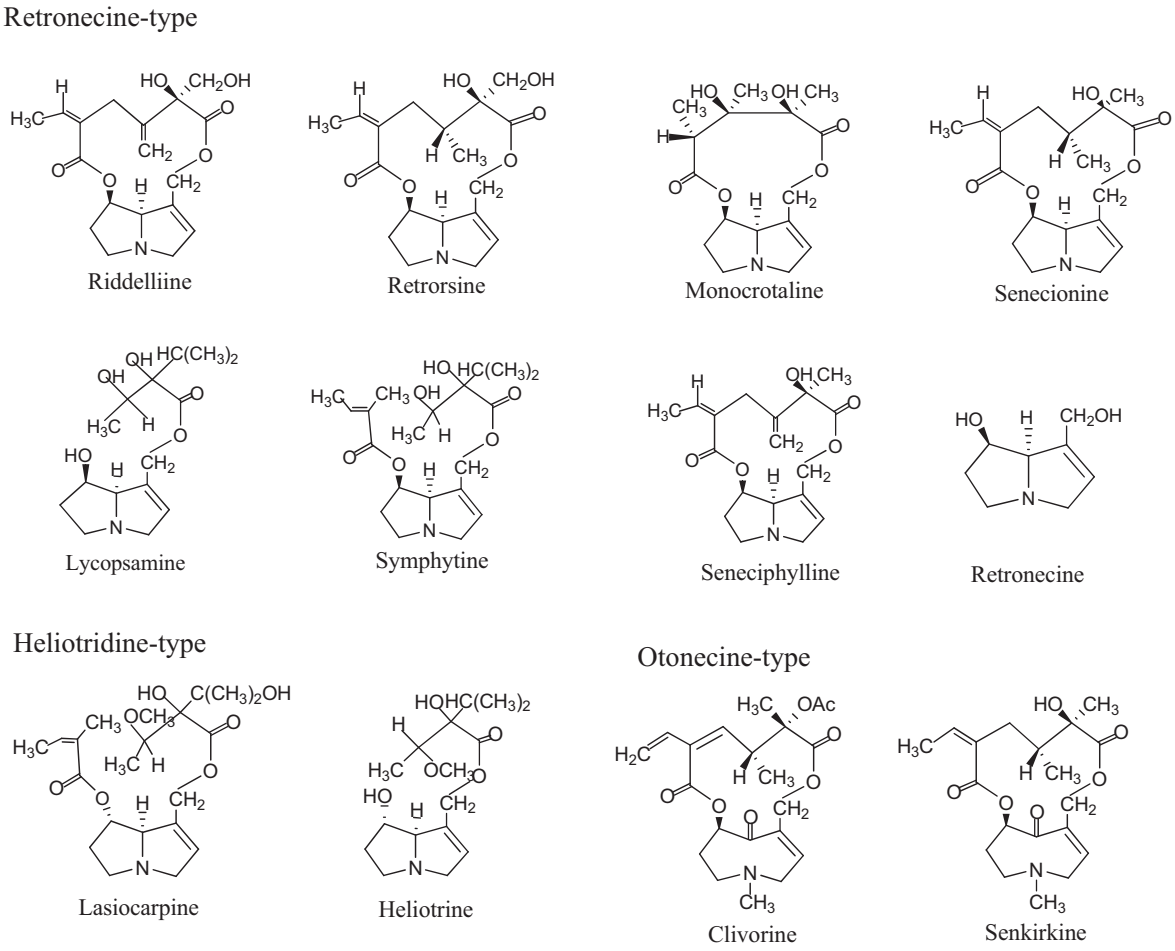

Fig. 1. Names and structures of representative tumorigenic PAs.

are chemically and biologically very reactive, capable of binding cellular macromolecules, such as protein and DNA, to generate DNA adducts, protein adducts and DNA and protein cross-links to exert toxicity, including hepatotoxicity, tumorigenicity, mutagenicity, and teratogenicity (Fig. 2). Dehydro-PAs can also bind to one or two molecules of glutathione to form glutathione conjugates for excretion, or are hydrolyzed into (±)-6,7-dihydro-7-hydroxy-1-hydroxymethyl-5*H*-pyrrolizine (DHP) (Fig. 2).

The mechanism by which PAs induce tumors was not known for about 50 years until we reported in 2001 that riddelliine, one of the tumorigenic PAs, induced liver tumors through a genotoxic mechanism mediated by the formation of DHP-derived DNA adducts (Yang et al., 2001). Subsequent studies on riddelliine and other PAs showed that DHP-derived DNA adducts were also formed from metabolism of other tumorigenic PAs *in vivo* and *in vitro* (Chou et al., 2003; Chou and Fu, 2006; Fu et al., 2004, 2007, 2010; Xia et al., 2003, 2004, 2008). On the other hand, although it has been reported that PAs and dehydro-PAs can induce cancer in the skin (Rao and Reddy, 1978; Mattocks and Cabral, 1982), the mechanism is yet not known.

PAs have been shown to be the most important phytochemicals that, upon metabolism in the liver, can cause secondary (or hepatogenous) photosensitization in animals (Knight and Walter, 2003). It was proposed that the liver damaged by PAs is unable to eliminate phylloerythrin, which is a bacterial breakdown product of chlorophyll. When the accumulated phylloerythrin in the blood and skin is exposed to sunlight, the resulting fluorescent material can cause oxidative injury to the blood vessels and skin tissues (Clare, 1955). To date, the mechanism of causing phylloerythrin accumulation by PAs is not known. Since dehydro-PAs are highly reactive, we propose that when they circulate to the skin, they can lead to photosensitization in the skin. Or, they may be metabolically formed in the skin, eliciting skin tumors by a phototoxic effect.

As a continuation of our studies, we investigated the phototoxicity of a series of parent PAs and their metabolites under UVA irradiation. These include five parent PAs (riddelliine, monocrotaline, retrorsine, lasiocarpine, and senkirkine); four PA *N*-oxides (riddelliine *N*-oxide, monocrotaline *N*-oxide, retrorsine *N*-oxide, and heliotrine *N*-oxide); seven dehydro-PAs (dehydroriddelliine, dehydromonocrotaline, dehydroretrorsine, dehydrosenecionine, dehydroseneciphylline, dehydrolasiocarpine and dehydroheliotrine), retronecine, dehydroretronecine (DHR), 7-(deoxyguanosin-N^2-yl)dehydrosupinidine (DHP-dG-1), and 7-glutathionyl-6,7-dihydro-1-hydroxymethyl-5*H*-pyrrolizine (7-GSH-DHP). DHP-dG-1 is one of the PA-derived DNA adduct detected *in vitro* and *in vivo* (Fu et al., 2010) and 7-GSH-DHP is a metabolite of PAs formed *in vivo* (Lin et al., 2000). DHP is a racemic mixture and DHR is its enantiomer with the 7-hydroxyl group possessing an R-absolute configuration. We found that, in the presence of a lipid (methyl linoleate), while all the dehydro-PAs and 7-GSH-DHP induced lipid peroxidation, all the parent PAs and the other metabolites did not. Mechanistic studies, both with free radical inhibitors and enhancers and with electron spin resonance (ESR) spin trapping techniques, revealed that UVA photoirradiation of these compounds generated reactive oxygen species (ROS) that mediated the initiation of lipid peroxidation.

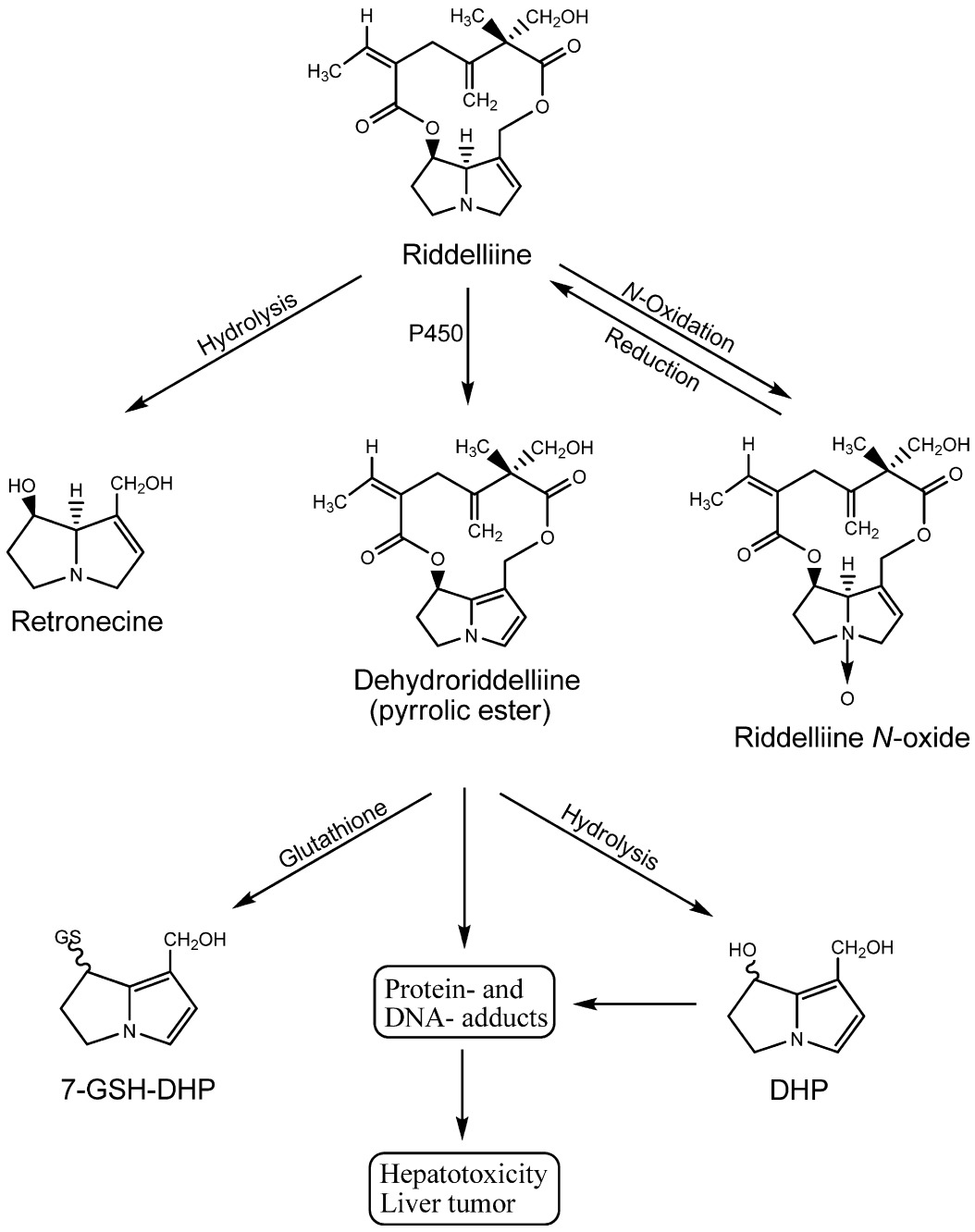

Fig. 2. Metabolism of riddelliine leading to hepatotoxicity, tumorigenicity, and GSH-DHP adducts.

2. Materials and methods

2.1. Materials

Monocrotaline, retrorsine, retrorsine *N*-oxide, glutathione (GSH), *o*-bromanil (3,4,5,6-tetrabromo-*o*-benzoquinone), *o*-chloranil (3,4,5,6-tetrachloro-*o*-benzoquinone), methyl linoleate (ML), sodium azide (NaN_3), 1,2-dimethoxyethane, diethylene-triaminepentaacetic acid, superoxide dismutase (SOD), and 2,2,6,6-tetramethyl-piperidine (TEMP) were purchased from Sigma–Aldrich Chemical Co. (St. Louis, MO). Heliotrine was purchased from Accurate Chemical & Scientific Corporation (Westbury, NY). Riddelliine was a gift from Dr. Po-Chuen Chan, the US National Toxicology Program. Lasiocarpine was gift from Dr. John A. Edgar, CSIRO Livestock Industries, Australia (Xia et al., 2006). Senecionine and seneciphylline were a gift from Dr. Russell J. Molyneur, Western Regional Research Center, Agricultural Research Service, The US Department of Agriculture. Riddelliine *N*-oxide and monocrotaline *N*-oxide were synthesized as described previously (Wang et al., 2005). Heliotrine *N*-oxide was similarly prepared. The nitrone spin trap, 5-*tert*-butoxycarbonyl 5-methyl-1-pyrroline *N*-oxide (BMPO) was purchased from Applied Bioanalytical Labs (Sarasota, FL). AX® 1-X8 anion exchange resin was from BIO-RAD Laboratory (chloride form, 200 to 400 dry mesh) and was transformed into hydroxyl form (following the transformation instruction provided in the handbook with the product). All other reagents were obtained through commercial sources and were HPLC grade.

2.2. Preparation of dehydropyrrolizidine alkaloids, DHP-dG-1, and 7-GSH-DHP

Dehydromonocrotaline was synthesized following the method of Mattocks (Mattocks et al., 1989) with modification. Briefly, a solution of monocrotaline (1.0 g, 3.08 mmol), dissolved in 200 mL chloroform in a 500 mL round bottom flask and placed in an ice bath, was added dropwise 1.37 g *o*-bromanil (3.2 mmol) in 5 mL of cold chloroform with shaking. After the reaction mixture was agitated for 1–2 min, 60 g hydroxy form AX® 1-X8 anion exchange resin was introduced into the flask, followed with strong shaking. The reaction mixture was filtered through a Buchner funnel, followed by removal of the solvent (chloroform) under reduced pressure in a rotary evaporator. The resulting crude dehydromonocrotaline, a yellowish solid, was dissolved in ethyl ether. Upon filtration and removal of ethyl ether from the fil-

trate, dehydromonocrotaline was obtained as white solid in 920 mg (92% yield); m.p. 86–88 °C (dec.) (Culvenor et al., 1970, 85–90 °C); UV λ_{max} 235 nm (in 1,2-dimethoxyethane).

The other dehydro-PAs, dehydroriddelliine (86% yield), dehydroheliotrine (85% yield), dehydrolasiocarpine (75% yield), dehydroretrorsine (75% yield), dehydroseneciphylline (70% yield), and dehydrosenecionine (70% yield) were synthesized, either similarly to the preparation of dehydromonocrotaline described above, or used *o*-chloranil, followed by washing with hydroxy resin as described by Culvenor et al. (1970) or Kim et al. (1995). The identity and purity of all the synthesized dehydro-PAs were validated by UV–visible and LC/MS spectral analysis. These compounds kept cold (−20 °C) until used.

DHP-dG-1 and 7-GSH-DHP were prepared as previously described (Fu et al., 2010; Lin et al., 2000). DHR was prepared by barium hydroxide catalyzed hydrolysis of monocrotaline followed by dehydrogenation of the resulting retronecine with *o*-bromanil (Yang et al., 2001).

2.3. Light sources

The UVA light box was custom made using 4 UVA lamps (National Biologics, Twinsburg, OH) (Chiang et al., 2010). The spectral irradiance of the light box was determined using an Optronics OL754 Spectroradiometer (Optronics Laboratories, Orlando, FL), and the light dose was routinely measured using a Solar Light PMA-2110 UVA detector (Solar Light Inc., Philadelphia, PA). The maximum emission of the UVA light box was determined to be between 340 and 355 nm. The light intensities at wavelengths below 320 nm (UVB light) and above 400 nm (visible light) are approximately two orders of magnitude lower than the maximum in the 340–355 nm spectral region (Chiang et al., 2010).

For the UVA light-induced lipid peroxidation by PAs, their metabolites, and dG adduct, the UVA-irradiation doses were 14, 35, and 70 J/cm^2, which were obtained by approximately 46, 115, and 230 min exposure at the dose rate of 5 mW/cm^2. 10 J/cm^2 of UVA equates to about 2 h exposure at noon sunny summer days, based upon observations of UVA intensity of 3.6 mW/cm^2 in Jackson, MS, USA, in August (Yu et al., 2001) and 5.4 mW/cm^2 in Paris, France, in July (Jeanmougin and Civatte, 1987).

2.4. Photoirradiation of PAs, PA-N-oxides, retronecine, dehydro-PAs, DHR, 7-GSH-DHP, and DHP-dG-1 with UVA light in the presence of methyl linoleate

Experiments were conducted using a solution of 100 mM methyl linoleate and 0.1 mM PAs, dehydro-PAs, or other PA metabolites in methanol. Samples were placed in a UV-transparent cuvette and irradiated with 0, 14, 35, or 70 J/cm^2 of UVA light. After irradiation, the methyl linoleate hydroperoxide products were separated by HPLC using a Prodigy 5 μm ODS column (4.6 mm × 250 mm, Phenomenex, Torrance, CA) eluted isocratically with 10% water in methanol (v/v) at 1 mL/min. The levels of lipid peroxidation were determined by HPLC and were quantified by monitoring HPLC peak areas at 235 nm (Chiang et al., 2010) followed by conversion to concentrations based on the molar extinction coefficient (at 235 nm) reported by Gibian and Vandenberg (1987).

2.5. UVA light-induced lipid peroxidation by 7-GSH-DHP and dehydroriddelliine in the presence of a free radical scavenger or enhancer

The experiments were carried out as described above, with parallel experiments conducted in the presence of NaN_3 or SOD. The concentration of SOD was 200 U/mL and NaN_3 was 20 mM.

It has been established that the lifetime of singlet oxygen is longer in deuterated solvents, such as deuterated water or methanol, than in protic solvent (Ogilby and Foote, 1983). Photoirradiation of 7-GSH-DHP and dehydroriddelliine in the presence of CH_3OH and CH_3OD was studied similarly.

2.6. Detection of free radicals formed following photoexcitation of dehydromonocrotaline and dehydroriddelliine by electron spin resonance spectroscopy (ESR) with spin trapping

ESR with spin trapping was used to detect superoxide anion radicals ($O_2^{\bullet-}$) formed during photoexcitation of the alkaloid samples. Dehydromonocrotaline or dehydroriddelliine at 1.8 mM in 90% CH_3CN was mixed with 25 mM BMPO (Zhao et al., 2001) and transferred to a 50 μL quartz capillary tube. The capillary tube was placed into the microwave cavity of a Bruker EMX ESR Spectrometer (Billerica, MA). The tube was irradiated at 345 nm in the microwave cavity using light emitted from a 500 W Xe arc lamp directed through a McPherson monochromator, model DM200 (Chelmsford, MA). ESR spectra were collected during irradiation at 5, 12, 20, 30, and 40 min. All ESR measurements were carried out at ambient temperature (27 °C) using the following settings for detection of the spin adduct between BMPO and $O_2^{\bullet-}$ (BMPO–$^{\bullet}$OOH) (Rinalducci et al., 2004): 20 mW microwave power, 100 G scan range, 1 G field modulation amplitude, and 100 kHz modulation frequency. The data were obtained with errors of less than 10%.

For detection of singlet oxygen, samples containing 1.8 mM dehydromonocrotaline (or dehydroriddelliine) and 20 mM TEMP in 95% CH_3CN were irradiated at 340 nm, and ESR spectra were recorded after 20, 30, and 40 min of irradiation. Control samples did not contain any dehydromonocrotaline or dehydroriddelliine. The resulting typical ESR profile of TEMPO was determined according to previously published by Rinalducci et al. (2004). ESR instrument and instrument settings were identical to those used for detection of superoxide anion radicals.

2.7. Statistical analysis

Data are presented as mean ± SD. One-way analysis of variance (ANOVA) followed by pairwise-comparisons using Dunnett's *t*-tests was used to determine the significance of difference in photoinduced hydroperoxidation between samples with PA metabolites and a control sample (methyl linoleate only). The difference was considered statistically significant when the *P* value was less than 0.05.

2.8. Instrumentation

For the separation and purification of the methyl linoleate hydroperoxide products, HPLC analysis was conducted on an Alliance™ HPLC system consisting of Waters 2690 Separations Module and a Waters 996 diode array spectrophotometric detector. For organic synthesis, adducts (DHP-dG-1 and 7-GSH-DHP) were separated on a Waters HPLC system consisting of Waters 600 pump and controller and a Waters 996 diode array spectrophotometric detector.

LC/MS conditions. A Shimadzu HPLC system, consisting of a SCL-10Avp controller, a SPD-M10Avp photodiode array detector, and 2 Shimadzu LC-10ADvp pumps, was used for the analysis of the dehydro-PAs and DHP-dG adducts.

3. Results

3.1. Photoirradiation of PAs, PA-N-oxides, dehydro-PAs, retronecine, DHR, 7-GSH-DHP, and DHP-dG-1 in the presence of methyl linoleate

Photoirradiation of PAs in methanol with UVA light in the presence of methyl linoleate was studied to determine whether photoirradiation of PAs can initiate lipid peroxidation. Photoirradiation of 100 mM methyl linoleate alone, and a mixture of 100 mM methyl linoleate and 0.1 mM monocrotaline with 0, 14, 35, and 70 J/cm^2 of UVA light were conducted in parallel. The extent of lipid peroxide formation following irradiation was measured by calculation of the amount of methyl linoleate hydroperoxide based on the HPLC peak areas detected at 235 nm. Comparison of the results of methyl linoleate hydroperoxide formation with those from controls (photoirradiation of methyl linoleate alone) indicated that photoirradiation of monocrotaline did not generate lipid peroxidation significantly higher than the control (Table 1).

Table 1
UVA photoirradiation of 0.1 mM PAs, PA *N*-oxides, dehydro-PAs, retronecine, DHR, DHP-dG-1, and 7-GSH-DHP in the presence of methyl linoleate. Data are expressed as means ± SD ($n = 3$).

Chemical	Methyl linoleate hydroperoxide (mM)		
	UVA 14 J/cm^2	UVA 35 J/cm^2	UVA 70 J/cm^2
Methyl linoleate (ML)	2.83 ± 0.24	4.02 ± 0.35	6.84 ± 0.81
Dehydromonocrotaline	9.32 ± 0.30	21.22 ± 0.65	37.51 ± 5.28
Dehydroriddelliine	10.24 ± 0.74	21.47 ± 1.56	37.37 ± 6.89
Dehydroheliotrine	9.05 ± 0.89	19.53 ± 1.62	34.41 ± 1.86
Dehydrolasiocarpine	7.40 ± 0.11	15.59 ± 0.99	27.53 ± 0.91
Dehydroretrorsine	9.34 ± 0.20	18.47 ± 0.11	31.51 ± 0.66
Dehydrosenecionine	8.91 ± 0.34	18.46 ± 0.63	30.49 ± 0.15
Dehydroseneciphylline	8.48 ± 0.05	18.62 ± 0.34	30.79 ± 2.49
DHR	2.27 ± 0.25	2.90 ± 0.53	4.60 ± 1.41
Monocrotarline	4.07 ± 0.34	4.78 ± 0.59	5.83 ± 0.29
Riddelliine	4.02 ± 0.34	4.84 ± 0.44	6.65 ± 0.35
Heliotrine	4.50 ± 0.30	5.92 ± 0.65	8.04 ± 1.10
Retronecine	4.18 ± 0.27	5.06 ± 0.52	6.45 ± 0.82
Lasiocarpine	3.91 ± 0.23	5.32 ± 0.27	7.01 ± 0.64
Senkirkine	3.65 ± 0.29	4.13 ± 0.29	5.62 ± 0.38
Monocrotaline *N*-oxide	2.89 ± 0.21	4.06 ± 0.47	6.75 ± 0.37
Riddelliine *N*-oxide	2.98 ± 0.18	3.95 ± 0.28	6.58 ± 0.46
Heliotrine *N*-oxide	3.32 ± 0.42	3.96 ± 0.22	6.31 ± 0.57
Retrornecine *N*-oxide	2.60 ± 0.24	3.12 ± 0.34	6.14 ± 0.63
7-GSH-DHP	7.43 ± 0.95	17.41 ± 2.42	33.29 ± 0.43
DHP-dG-1	2.33 ± 0.21	2.80 ± 0.54	3.70 ± 0.59

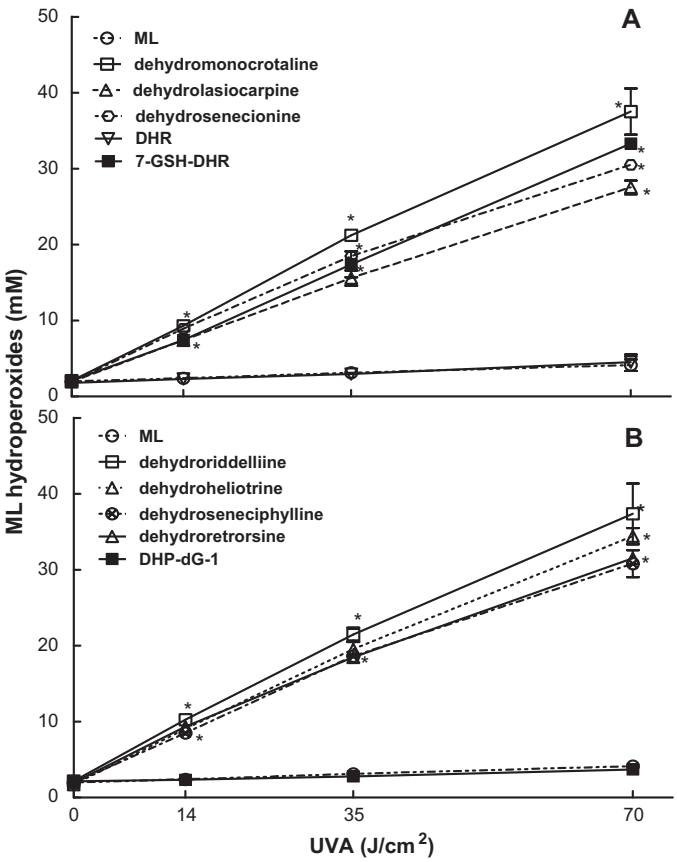

Fig. 3. Induction of lipid peroxidation by photoirradiation of seven 0.1 mM dehydro-PAs (dehydromonocrotaline, dehydroriddelliine, dehydroheliotrine, dehydroretrosine, dehydrosenecionine, dehydroseneciphylline, and dehydrolasiocarpine), DHR, 7-GSH-DHP, and DHP-dG-1 in methanol in the presence of methyl linoleate (ML) with UVA light at light dose of 0, 35, and 70 J/cm^2, respectively. The levels of peroxidation were measured by HPLC monitored at 235 nm. The symbol * indicates significant difference from control (ML only) ($p < 0.05$).

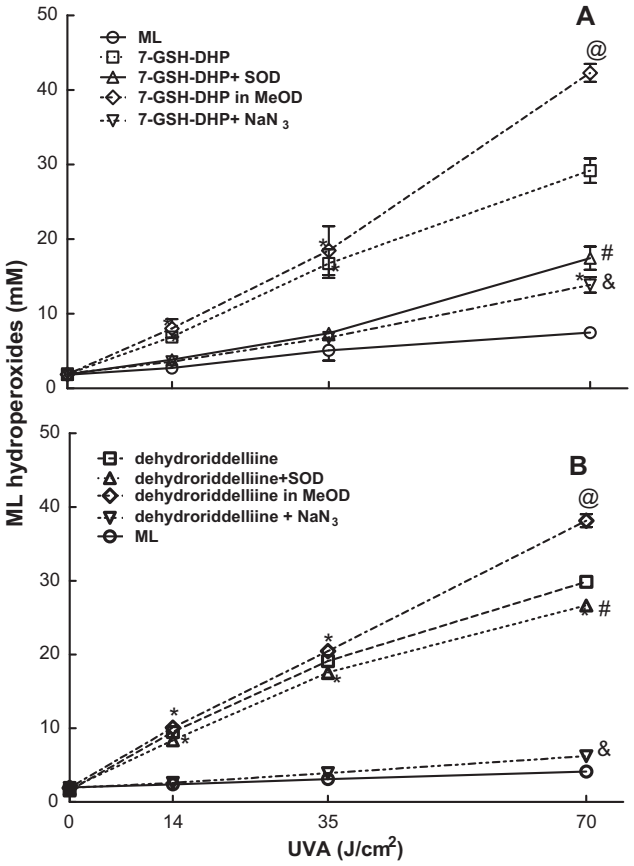

Fig. 4. Effects of deuterated methanol, NaN_3, and SOD on peroxidation of methyl linoleate initiated by UVA photoirradiation of 0.1 mM (A) 7-GSH-DHP and (B) dehydroriddelliine. The levels of peroxidation were measured by HPLC monitoed at 235 nm. The symbol * indicate significant difference from negative control ($p < 0.05$). The symbols @, #, and & indicate significant difference between the groups with and without a free radical scavenger or an enhancer ($p < 0.05$).

UVA photoirradiation of other four parent PAs (riddelliine, lasiocarpine, heliotrine, and senkirkine), seven dehydro-PAs, four PA *N*-oxides, retronecine, DHR, 7-GSH-DHP, and DHP-dG-1 was conducted under similar experimental conditions (Table 1). Similar to monocrotaline, all the parent PAs, the four PA *N*-oxides, retronecine, DHR, and DHP-dG-1 did not induce lipid peroxidation significantly higher than the control (methyl linoleate) (Table 1).

On the other hand, the seven dehydro-PAs, including dehydromonocrotaline, dehydroriddelliine, dehydroheliotrine, dehydrolasiocarpine, dehydroretrorsine, dehydroseneciphylline, and dehydrosenecionine, as well as 7-GSH-DHP, induced lipid peroxidation significantly higher than the control, and in a light dose-dependent manner (Table 1 and Fig. 3).

3.2. Peroxidation of methyl linoleate initiated by photoirradiation of dehydroriddelliine and 7-GSH-DHP in the presence of a free radical scavenger or CH_3OD

The involvement of free radical intermediates in the photoinduced peroxidation of methyl linoleate in the presence of dehydroriddelliine and 7-GSH-DHP was examined. The superoxide free radical scavengers SOD and NaN_3 were employed for study. NaN_3 is a common free radical scavenger especially for singlet oxygen ($^1O_2$) (Basu-Modak and Tyrrell, 1993) and hydroxyl radical ($^{\bullet}OH$) (Sortino et al., 1998). Because singlet oxygen has a longer half-life in deuterium solvents (Ogilby and Foote, 1983), methanol was replaced by CH_3OD to determine whether or not lipid peroxidation would be enhanced.

The results shown in Fig. 4A clearly indicated that peroxidation of methyl linoleate by 7-GSH-DHP was significantly ($P \leq 0.05$) inhibited by NaN_3 and SOD as compared to the photoirradiation of 7-GSH-DHP. On the other hand, replacement of CH_3OH by CH_3OD significantly ($P \leq 0.05$) enhanced peroxidation (Fig. 4A) at a light dose of 70 J/cm^2. These results suggested that both singlet oxygen and superoxide free radical were involved in lipid peroxidation by photoirradiation of 7-GSH-DHP.

Similar inhibition and enhancement results were found in the photoirradiation of dehydroriddelliine (Fig. 4B). The overall results suggested that UVA photoirradiation of 7-GSH-DHP and dehydroriddelliine generated singlet oxygen and superoxide, both of which initiated lipid peroxidation.

3.3. Detection of reactive oxygen species (ROS) using ESR

To confirm further the involvement of ROS in the induction of lipid peroxidation from UVA photoirradiation of dehydro-PAs and 7-GSH-DHP, the ERS spin trapping technique was employed to determine whether or not UVA photoirradiation of dehydromonocrotaline and dehydroriddelliine generates singlet oxygen and/or superoxide.

The commonly used specific spin trap TEMP was employed for probing singlet oxygen formation (Lion et al., 1976; Xia et al., 2006). In the study, a solution ($CH_3CN/H_2O = 95/5$) of 1.8 mM dehydromonocrotaline (or dehydroriddelliine) containing 20 mM

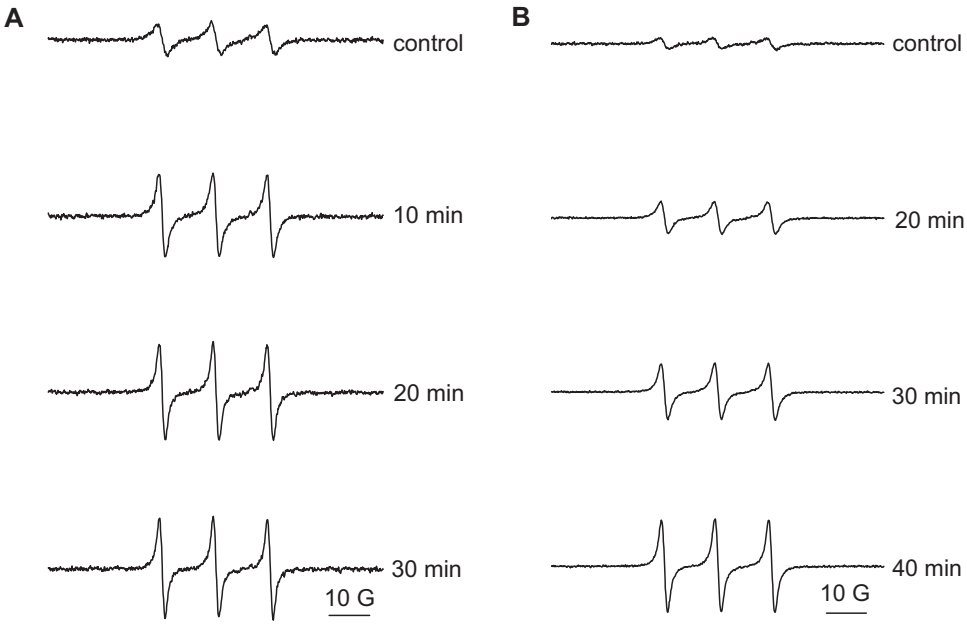

Fig. 5. (A) A solution of 1.8 mM dehydromonocrotaline and 20 mM TEMP-1 in 95% CH_3CN was irradiated at 340 nm, and ESR signals were recorded after 10, 20, and 30 min exposure. (B) A solution of 1.8 mM dehydroriddelliine and 20 mM TEMP-1 in 95% CH_3CN was irradiated at 340 nm, and ESR signals were recorded after 20, 30, and 40 min exposure. ESR instrument settings were as follows: 20 mW microwave power, 100 G sweep width, 1 G field modulation amplitude, and 100 kHz modulation frequency.

TEMP was photoirradiated under UVA at wavelength of 340 nm. Upon UVA irradiation for 5 min, singlet oxygen was generated and trapped by TEMP to produce an ESR spectral profile which is typical of TEMPO (data not shown) (Rinalducci et al., 2004). The intensity of these ESR signals progressively enhanced when photoirradiation time increased from 5 up to 30 min (Fig. 5A). These results provided direct evidence that photoirradiation of dehydromonocrotaline with UVA light generated singlet oxygen and that the quantity of singlet oxygen formed was dependent on the light dose.

A study with dehydroriddelliine was conducted similarly. Upon exposure to UVA light up to 40 min, singlet oxygen was generated, with the intensity of TEMPO ESR signals progressively enhanced (Fig. 5B). These results provided direct evidence that photoirradiation of dehydroriddelliine with UVA light generated singlet oxygen and that the quantity of singlet oxygen formed was dependent on the light dose.

To determine whether or not photoirradiation of dehydromonocrotaline with UVA light generates superoxide radical anion, BMPO, a trapping agent that efficiently traps superoxide radical anion (Rinalducci et al., 2004), was employed. The advantage of BMPO is that once BMPO-superoxide adduct (i.e., BMPO–•OOH) is formed from reaction of BMPO with superoxide radical anion, the resulting adduct is highly stable and does not decompose into the corresponding hydroxyl adduct (i.e., BMPO–•OH) (Rinalducci et al., 2004).

Photoirradiation of dehydromonocrotaline with UVA light (345 mm) in the presence BMPO for 5 min produced ESR spectral signals (Fig. 6A). The ESR spectral profiles were typical of BMPO–•OOH (Xia et al., 2006), confirming that the generated ESR profile was identical to that of BMPO-superoxide adduct (i.e., BMPO–•OOH). Similar to the formation of singlet oxygen, the intensity of these ESR signals progressively increased when photoirradiation time increased to 12, 20, 30, and 40 min (Fig. 6A). These results provided direct evidence that superoxide radical anion was generated from photoirradiation of dehydromonocrotaline by UVA light and that the quantity of superoxide radical anion formed was dependent on the light dose.

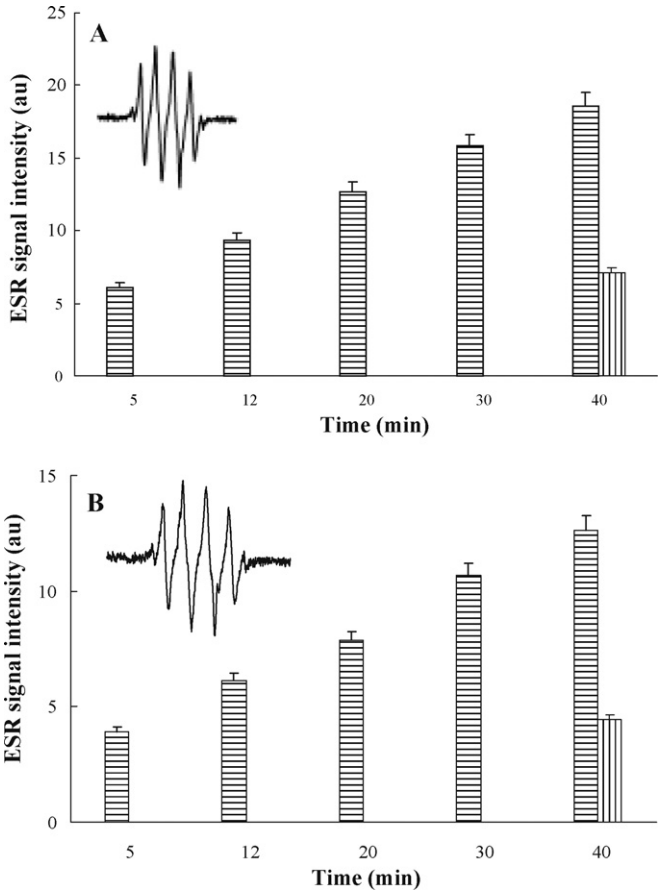

Fig. 6. A solution of 1.8 mM (A) dehydromonocrotaline and (B) dehydroriddelliine and 25 mM BMPO in 90% CH_3CN was irradiated at 345 nm, and ESR signals were recorded after different time intervals. ESR instrument settings were as follows: 20 mW microwave power, 100 G sweep width, 1 G field modulation amplitude, and 100 kHz modulation frequency. (A and B) The shorter bar at 40 min was the experiment with SOD (500 units) incorporated into the reaction mixture.

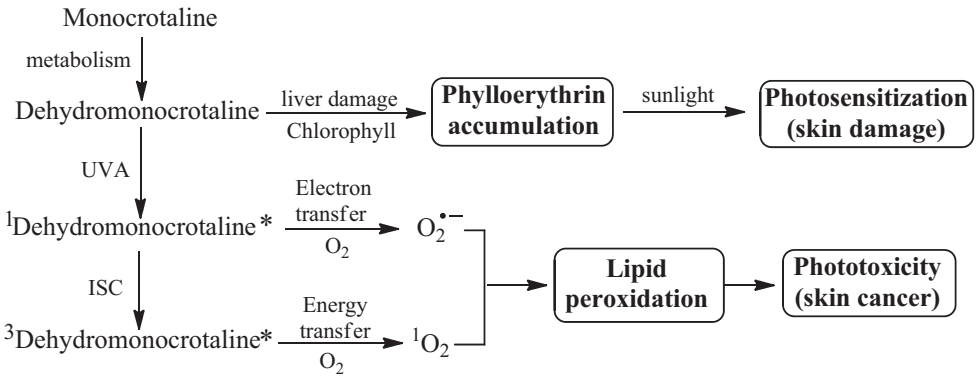

Fig. 7. Proposed mechanism of lipid peroxidation by dehydromonocrotaline under UVA irradiation.

Similar results were obtained from photoirradiation of dehydroriddelliine, the intensity of ESR signals progressively increased when photoirradiation time increased from 5 to 12, 20, 30, and 40 min (Fig. 6B). These results confirmed that superoxide radical anion was generated from photoirradiation of dehydroriddelliine with UVA light and that the quantity of superoxide radical anion formed is dependent on the light dose. The only difference from the photoirradiation of dehydroriddelliine was that the intensities of ESR signals from photoirradiation of dehydroriddelliine were weaker than those from dehydromonocrotaline.

4. Discussion

Liver metabolism of PAs generate PA *N*-oxides, retronecine, DHP, and dehydro-PAs as primary metabolites. Dehydro-PAs are highly reactive, capable of reacting with cellular DNA and protein to form DNA adducts, protein adducts, and DNA–DNA and DNA-protein adducts, resulting in hepatotoxicity, mutagenicity, teratogenicity, and tumorigenicity (Fu et al., 2010; IARC, 1976; Mattocks, 1986). In the present study, we demonstrated that upon UVA irradiation, dehydro-PAs can generate ROS leading to induction of lipid peroxidation. This is the first demonstration of the UVA-induced phototoxic activity exerted by dehydro-PAs in contrast to their well-known metabolism-dependent adverse effects. We determined the mechanism of lipid peroxidation mediated by ROS by two distinct approaches. The involvement of singlet oxygen in UVA light-induced lipid peroxidation by dehydroriddelliine and 7-GSH-DHP was determined by the inhibition effect by sodium azide and the enhancement by deuterated methanol (Fig. 4). The inhibition of lipid peroxidation by superoxide dismutase suggested that lipid peroxidation was mediated by superoxide (Fig. 4). Furthermore, the formation of single oxygen and superoxide from UVA photoirradiation of dehydroriddelliine and dehydromonocrotaline was validated by ESR spin trapping studies (Figs. 5 and 6).

Based on the results, a mechanism of UVA photoirradiation of dehydro-PAs leading to formation of singlet oxygen and superoxide and induction of lipid peroxidation is proposed (Fig. 7). Taking photoirradiation of dehydromonocrotaline as an example, upon UVA irradiation, dehydromonocrotaline is photoexcited to form dehydromonocrotaline* which serves as the initiating species and is found in both the excited singlet state (^{1}dehydromonocrotaline*) and excited triplet state (^{3}dehydromonocrotaline*). The excited singlet state of dehydromonocrotaline (^{1}dehydromonocrotaline*) transfers an electron to molecular oxygen to generate superoxide radical anion (Type I mechanism) (Foote, 1991). The excited triplet of dehydromonocrotaline (^{3}dehydromonocrotaline*) can transfer energy to molecular oxygen to generate singlet oxygen (Type II mechanism) (Foote, 1991). In the presence of a lipid, both the generated superoxide radical anion and singlet oxygen can initiate the lipid peroxidation leading to PA-associated phototoxicity.

It is well established that both ROS and lipid peroxidation in humans are associated with many age-related diseases including cancer, athereosclerosis, ischemia, inflammation, liver injury, and aging (Floyd et al., 2001; Stadtman and Berlett, 1997). Skin is the organ that can concomitantly be exposed to both dehydro-PAs and light. The results from this study suggest that when dehydro-PAs are present in the skin, they can induce phototoxicity, via generation of ROS and lipid peroxidation, leading to enhancing skin damage, including skin cancer.

PAs can cause secondary (hepatogenous) photosensitization in animals (Knight and Walter, 2003). By definition, secondary (hepatogenous) photosensitization agents require metabolism in the liver and the reactive metabolites cause photosensitization in the skin. This is different from the primary photosensitization agents, such as St. John's wort, which upon uptake, circulate to the skin, expose to UV light, fluoresce, and cause skin damage (Knight and Walter, 2001).

To date, the cause of photosensitization by PAs is not clear. It was proposed that the liver damaged by PAs is unable to eliminate phylloerythrin, which is a breakdown product of chlorophyll. When the accumulated phylloerythrin in the blood and skin is exposed to sunlight, the resulting fluorescent material can cause oxidative injury to the blood vessels and skin tissues (Clare, 1955). From our study, among all the PAs and PA metabolites so far tested, dehydro-PAs and the 7-GSH-DHP adduct are the compounds exhibiting phototoxicity. Thus, on the basis of our present results, we propose that there are three pathways that dehydro-PAs and 7-GSH-DHP adduct can cause photosensitization in the skin. The first pathway is that dehydro-PAs and 7-GSH-DHP formed in the liver are trans-located to the skin, and on exposure to light, lead to skin damage (Fig. 7). The second pathway is that PAs circulate to the skin and skin can metabolize PAs to the corresponding dehydro-PA metabolites leading to photosensitization (Fig. 7). The third pathway is that dehydro-PAs can cause liver damage, leading to phylloerythrin accumulation in the blood and skin, and skin damage (photosensitization) (Fig. 7). All these proposed mechanisms warrant further investigation.

Conflict of interest

None.

Acknowledgments

We thank Drs. William Melchior and Frederick A. Beland for critical review of this manuscript and Dr. Lining Cai of Bioytanex Co. for mass spectral measurements of the pyrrolic metabolites and Dr.

Qiangen Wu for the statistical analysis of data. We also thank a gift of riddelliine from Dr. Po-Chuen Chan, of lasiocarpine from Dr. John A. Edgar, and of senecionine and seneciphylline from Dr. Russell J. Molyneur. This research was supported in part by appointment (Y. Zhao) to the Postgraduate Research Program at the NCTR administered by the Oak Ridge Institute for Science and Education through an interagency agreement between the US Department of Energy and the FDA.

References

Basu-Modak, S., Tyrrell, R.M., 1993. Singlet oxygen: a primary effector in the ultraviolet A/near-visible light induction of the human heme oxygenase gene. Cancer Res. 53, 4505–4510.

Chiang, H.M., Yin, J.J., Xia, Q.S., Zhao, Y.W., Fu, P.P., Wen, K.C., Yu, H.T., 2010. Photoirradiation of azulene and guaiazulene—formation of reactive oxygen species and induction of lipid peroxidation. J. Photochem. Photobiol. A 211, 123–128.

Chou, M.W., Fu, P.P., 2006. Formation of DHP-derived DNA adducts in vivo from dietary supplements and chinese herbal plant extracts containing carcinogenic pyrrolizidine alkaloids. Toxicol. Ind. Health 22, 321–327.

Chou, M.W., Yan, J., Nichols, J., Xia, Q., Beland, F.A., Chan, P.-C., Fu, P.P., 2003. Correlation of DNA adduct formation and riddelliine-induced liver tumorigenesis in F344 rats and B6C3F(1) mice. Cancer Lett. 193, 119–125.

Clare, N.T., 1955. Photosensitization in animals. Adv. Vet. Sci., 182–211.

Culvenor, C., Edgar, J., Smith, L., Tweeddale, H., 1970. Dihydropyrrolizines. III. Preparation and reactions of derivatives related to pyrrolizidine alkaloids. Aust. J. Chem. 23, 1853–1867.

Floyd, R.A., West, M., Hensley, K., 2001. Oxidative biochemical markers; clues to understanding aging in long-lived species. Exp. Gerontol. 36, 619–640.

Foote, C.S., 1991. Definition of Type I and Type II photosensitized oxidation. J. Photochem. Photobiol. 54, 659–1659.

Fu, P.P., Chou, M.W., Churchwell, M., Wang, Y., Zhao, Y., Xia, Q., Gamboa da Costa, G., Marques, M.M., Beland, F.A., Doerge, D.R., 2010. High-performance liquid chromatography electrospray ionization tandem mass spectrometry for the detection and quantitation of pyrrolizidine alkaloid-derived DNA adducts in vitro and in vivo. Chem. Res. Toxicol. 23, 637–652.

Fu, P.P., Xia, Q., Lin, G., Chou, M.W., 2004. Pyrrolizidine alkaloids—genotoxicity, metabolism enzymes, metabolic activation, and mechanisms. Drug Metab. Rev. 36, 1–55.

Fu, P.P., Xia, Q.S., Chou, M.W., Lin, G., 2007. Detection, hepatotoxicity, and tumorigenicity of pyrrolizidine alkaloids in Chinese herbal plants and herbal dietary supplements. J. Food Drug Anal. 15, 400–415.

Fu, P.P., Yang, Y.C., Xia, Q.S., Chou, M.W., Cui, Y.Y., Lin, G., 2002. Pyrrolizidine alkaloids—tumorigenic components in Chinese herbal medicines and dietary supplements. J. Food Drug Anal. 10, 198–211.

Gibian, M.J., Vandenberg, P., 1987. Product yield in oxygenation of linoleate by soybean lipoxygenase: the value of the molar extinction coefficient in the spectrophotometric assay. Anal. Biochem. 163, 343–349.

International Agency for Research in Cancer (IARC), 1976. Pyrrolizidine alkaloids. In: IARC Monograph on the Evaluation of Carcinogenic Risk of Chemicals to Man—Some Naturally Occurring Substance. International Agency for Research in Cancer, Lyon, France.

International Programme on Chemical Safety (IPCS), 1989. Pyrrolizidine Alkaloids Health and Safety Guide. Health and Safety Criteria Guide, 26. WHO, Geneva.

Jeanmougin, M., Civatte, J., 1987. Dosimetry of solar ultraviolet radiation. Daily and monthly changes in Paris. Ann. Dermatol. Venereol. 114, 671–676.

Kim, H.Y., Stermitz, F.R., Coulombe Jr, R.A., 1995. Pyrrolizidine alkaloid-induced DNA-protein cross-links. Carcinogenesis 16 (11), 2691–2697.

Knight, A.P., Walter, R.G., 2001. A Guide to Plant Poisoning of Animals in North America. Teton NewMedia, Jackson Wyoming, pp. 142–150.

Knight, A.P., Walter, R.G., 2003. Plants affecting the skin and liver. In: A Guide to Plant Poisoning of Animals in North America. Teton NewMedia, Jackson, WY.

Li, S.L., Lin, G., Fu, P.P., Chan, C.L., Li, M., Jiang, Z.H., Zhao, Z.Z., 2008. Identification of five hepatotoxic pyrrolizidine alkaloids in a commonly used traditional Chinese medicinal herb, *Herba Senecionis scandentis* (Qianliguang). Rapid Commun. Mass Spectrom. 22, 591–602.

Lin, G., Cui, Y.-Y., Hawes, E.M., 2000. Characterization of rat liver microsomal metabolites of clivorine, an hepatotoxic otonecine-type pyrrolizidine alkaloid. Drug Metab. Dispos. 28, 1475–1483.

Lion, Y., Delmelle, M., van de Vorst, A., 1976. New method of detecting singlet oxygen production. Nature 263, 442–443.

Mattocks, A.R., Cabral, J.R., 1982. Carcinogenicity of some pyrrolic pyrrolizidine alkaloid metabolites and analogues. Cancer Lett. 17, 61–66.

Mattocks, A.R., 1986. Chemistry and Toxicology of Pyrrolizidine Alkaloids. Academic Press, London, NY.

Mattocks, A.R., Jukes, R., Brown, J., 1989. Simple procedures for preparing putative toxic metabolites of pyrrolizidine alkaloids. Toxicon 27, 561–567.

Ogilby, P.R., Foote, C.S., 1983. Chemistry of singlet oxygen. 42. Effect of solvent, solvent isotopic substitution and temperature on the lifetime of singlet molecular oxygen. J. Am. Chem. Soc. 105, 3423–3430.

Rao, M.S., Reddy, J.K., 1978. Malignant neoplasms in rats fed lasiocarpine. Br. J. Cancer 37, 289–293.

Rinalducci, S., Pedersen, J.Z., Zolla, L., 2004. Formation of radicals from singlet oxygen produced during photoinhibition of isolated light-harvesting proteins of photosystem II. Biochim. Biophys. Acta 1608, 63–73.

Roeder, E., 1995. Medicinal plants in Europe containing pyrrolizidine alkaloids. Pharmazie 50, 83–98.

Roeder, E., 2000. Medicinal plants in China containing pyrrolizidine alkaloids. Pharmazie 55, 711–726.

Smith, L.W., Culvenor, C.C.J., 1981. Plant sources of hepatotoxic pyrrolizidine alkaloids. J. Nat. Prod. 44, 129–152.

Sortino, S., Condorelli, G., de Guidi, G., Giuffrida, S., 1998. Molecular mechanism of photosensitization XI. Membrane damage and DNA cleavage photoinduced by Enoxacin. Photochem. Photobiol. 68, 652–659.

Stadtman, E.R., Berlett, B.S., 1997. Reactive oxygen-mediated protein oxidation in aging and disease. Chem. Res. Toxicol. 10, 485–494.

Wang, Y.-P., Yan, J., Fu, P.P., Chou, M.W., 2005. Human liver microsomal reduction of pyrrolizidine alkaloid *N*-oxide to form the corresponding carcinogenic parent alkaloid. Toxicol. Lett. 155, 411–420.

World Health Organization (WHO), 1988. Pyrrolizidine Alkaloids. International Programme on Chemical Safety Environmental Health Criteria 80. Environmental Health Criteria (EHC) Monographs, p. 337.

Xia, Q., Chou, M.W., Edgar, J.A., Doerge, D.R., Fu, P.P., 2006. Formation of DHP-derived DNA adducts from metabolic activation of the prototype heliotridine-type pyrrolizidine alkaloid, lasiocarpine. Cancer Lett. 231, 138–145.

Xia, Q., Chou, M.W., Lin, G., Fu, P.P., 2004. Metabolic formation of DHP-derived DNA adducts from a representative otonecine type pyrrolizidine alkaloid clivorine and the extract of Ligularia hodgsonnii hook. Chem. Res. Toxicol. 17, 702–708.

Xia, Q., Yan, J., Chou, M.W., Fu, P.P., 2008. Formation of DHP-derived DNA adducts from metabolic activation of the prototype heliotridine-type pyrrolizidine alkaloid, heliotrine. Toxicol. Lett. 178, 77–82.

Xia, Q.S., Chou, M.W., Kadlubar, F.F., Chan, P.C., Fu, P.P., 2003. Human liver microsomal metabolism and DNA adduct formation of the tumorigenic pyrrolizidine alkaloid, riddelliine. Chem. Res. Toxicol. 16, 66–73.

Yang, Y.C., Yan, J., Doerge, D.R., Chan, P.C., Fu, P.P., Chou, M.W., 2001. Metabolic activation of the tumorigenic pyrrolizidine alkaloid, riddelliine, leading to DNA adduct formation in vivo. Chem. Res. Toxicol. 14, 101–109.

Yu, H.B., Jin, W., Ho, H.L., Chan, K.C., Chan, C.C., Demokan, M.S., Stewart, G., Culshaw, B., Liao, Y.B., 2001. Multiplexing of optical fiber gas sensors with a frequency-modulated continuous-wave technique. Appl. Opt. 40, 1011–1020.

Zhao, H., Joseph, J., Zhang, H., Karoui, H., Kalyanaraman, B., 2001. Synthesis and biochemical applications of a solid cyclic nitrone spin trap: a relatively superior trap for detecting superoxide anions and glutathiyl radicals. Free Radic. Biol. Med. 31, 599–606.

Zhou, Y., Li, N., Choi, F.F.K., Qiao, C.F., Song, J.Z., Li, S.L., Liu, X., Cai, Z.W., Fu, P.P., Lin, G., Xu, H.X., 2010. A new approach for simultaneous screening and quantification of toxic pyrrolizidine alkaloids in some potential pyrrolizidine alkaloid-containing plants by using ultra performance liquid chromatography-tandem quadrupole mass spectrometry. Anal. Chim. Acta 681, 33–40.